THE OXIDATION OF ORGANIC COMPOUNDS IN THE TROPOSPHERE AND THEIR GLOBAL WARMING POTENTIALS

W. J. COLLINS [1], R. G. DERWENT [1], C. E. JOHNSON [2] and D. S. STEVENSON [3]

[1] *Climate Research Division, Meteorological Office, Bracknell, U.K.*
[2] *Hadley Centre for Climate Prediction and Research, Meteorological Office, Bracknell, U.K.*
[3] *Department of Meteorology, University of Edinburgh, Edinburgh, U.K.*

Abstract. Oxidation by hydroxyl radicals is the main removal process for organic compounds in the troposphere. This oxidation acts as a source of ozone and as a removal process for hydroxyl and peroxy radicals, thereby reducing the efficiency of methane oxidation and promoting the build-up of methane. Emissions of organic compounds may therefore lead to the build-up of two important radiatively-active trace gases: methane and ozone. Emission pulses of 10 organic compounds were followed in a global 3-D Lagrangian chemistry-transport model to quantify their indirect greenhouse gas impacts through changes induced in the tropospheric distributions of methane and ozone. The main factors influencing the global warming potentials of the 10 organic compounds were found to be their spatial emission patterns, chemical reactivity and transport, molecular complexity and oxidation products formed. The indirect radiative forcing impacts of organic compounds may be large enough that ozone precursors should be considered in the basket of trace gases through which policy-makers aim to combat global climate change.

1. Introduction

Oxidation by hydroxyl (OH) radicals is the main removal process for the organic compounds emitted by human activities and natural biogenic processes, although under some conditions, photolysis and reaction with nitrate radicals and halogen atoms may also be important (Atkinson, 2000). The rate of this OH-oxidation removal process depends on the hydroxyl radical concentration distribution, the concentration distribution of the organic compound (RH) and the rate coefficient for the reaction (1):

$$\mathrm{OH} + \mathrm{RH} = \text{oxidation products}\,. \tag{1}$$

For most organic compounds, this reaction (1) produces peroxy radicals (RO_2) (Atkinson, 2000) which in reaction (2), oxidise nitric oxide (NO) to nitrogen dioxide (NO_2), producing ozone (O_3), carbonyl products and a hydroperoxy (HO_2) radical through reactions (2)–(5) (Leighton, 1961; Demerjian et al., 1974):

$$\mathrm{RO_2} + \mathrm{NO} = \mathrm{NO_2} + \mathrm{RO} \tag{2}$$

$$\mathrm{RO} + \mathrm{O_2} = \mathrm{HO_2} + \text{carbonyl products} \tag{3}$$

Climatic Change **52:** 453–479, 2002.

$$NO_2 + h\nu = NO + O \tag{4}$$

$$O + O_2 + M = O_3 + M\,. \tag{5}$$

When there is sufficient NO under conditions of 'high-NO_x', the HO_2 radicals are efficiently recycled to OH (Logan, 1985), giving no overall radical loss following the oxidation of the organic compound, and the oxidation of organic compound leads to the production of O_3. There are, however, other reaction pathways involving RO_2 and HO_2 (Logan, 1985) which under 'low NO_x' conditions lead to the loss of peroxy radicals and hence hydroxyl radicals through reactions such as (6) and (7):

$$HO_2 + HO_2 + H_2O = H_2O_2 + O_2 + H_2O \tag{6}$$

$$RO_2 + HO_2 = ROOH + O_2 \tag{7}$$

or ozone destruction in reaction (8):

$$HO_2 + O_3 = OH + O_2 + O_2\,. \tag{8}$$

The loss of OH following the oxidation of organic compounds under 'low-NO_x' conditions means that as organic compounds build up, less OH is available to remove them and they build-up further in concentration (Isaksen and Hov, 1987).

An important implication of this increased competion for OH and decreased oxidation capacity is the enhanced build-up in methane concentrations. Methane is the second most important radiatively-active gas (IPCC, 1996) and its build-up is controlled by the oxidising capacity of the troposphere (Ehhalt, 1974). This feedback of methane growth upon methane concentrations adds an additional 20–70% to the methane build-up (IPCC, 1996). NO_x emissions play a crucial role also in fixing OH concentrations and hence in controlling methane concentrations, now and in the future (Kheshgi et al., 1999). The enhanced methane concentrations that result from emissions of organic compounds produce an indirect global warming (Johnson and Derwent, 1996). A side product of the oxidation of organic compounds under 'high-NO_x' conditions is the production of ozone, the third most important radiatively-active trace gas (IPCC, 1996). Emissions of organic compounds therefore produce an additional indirect global warming through enhanced ozone production to add to the methane indirect global warming (Johnson and Derwent, 1996).

To evaluate the total greenhouse effect generated by the emissions of a trace gas, the concept of global warming potential GWP has been defined (Derwent, 1990). To estimate GWPs, an understanding is required of how long the trace gas remains in the atmosphere and how it perturbs the global distributions of the major greenhouse gases. The total greenhouse effect is calculated by injecting an imaginary pulse of the trace gas into the atmosphere, simulating its decay and integrating its atmospheric burden and those of the major greenhouse gases over a time horizon

that is typically of the order of one hundred years. Prather (1994, 1996) and Wild and Prather (2000) have shown how this decay, for the case of methane, can be represented by a sum of exponential functions, the most important of which has an e-folding time of about 12 years. In the case of carbon monoxide CO, this same exponential decay is observed because the pulse of CO causes OH to decrease temporarily and methane to increase (Prather, 1996; Daniel and Solomon, 1998; Wild and Prather, 2000). In previous work (Derwent et al., 2001), we have shown that the emissions of a range of short-lived trace gases, including CO, oxides of nitrogen and hydrogen, can generate similar long-lived methane perturbations using a three-dimensional Lagrangian chemistry-transport model. This study extends our previous work to a range of organic compounds that are widely recognised as tropospheric ozone precursors by showing that they also generate similar long-lived methane perturbations.

2. Model Description

Following the oxidation of an organic compound with OH, the relative importance of OH loss, recycling or production depends on the local scale properties of the atmosphere, time-of-day, season and composition, and so the only way to account for all the processes is within a three-dimensional chemistry-transport model. The model employed in this study is the U.K. Meteorological Office STOCHEM model. This adopts a Lagrangian approach, using archived meteorological fields from the U.K. operational numerical weather prediction model (Cullen, 1993) to advect 50,000 constant mass air parcels around the globe in three dimensions in a domain extending up to 100 hPa with a three hour timestep. The large number of parcels allows the determination of species concentrations on a $5^\circ \times 5^\circ \times 100$ hPa grid.

The wind fields have been archived at 6-hourly intervals on a 1.25° longitude $\times$ 0.8333° latitude $\times$ 100 hPa grid. Sub-grid scale convective transport in our model is diagnosed using convective cloud fields and convective precipitation. The species concentrations in a fraction of the cells within a column below the convective cloud tops are completely mixed. Parcels are not expected to maintain their integrity indefinitely as they become distorted due to wind shears, so the mixing ratios are relaxed towards background values with a time constant depending on height. The background values are determined by the mean of neighbouring cells within a $5^\circ \times 5^\circ \times 100$ hPa grid.

Chemical species are emitted into the model on the above $5^\circ \times 5^\circ$ grid. Most are injected into the boundary layer that is in turn diagnosed from temperature and wind profiles. The emission rates of all the emitted species are listed in Table I, anthropogenic sources are constant throughout the year whilst natural biogenic sources vary monthly. Isoprene (C_5H_8) is emitted only during daylight hours at a rate governed by the solar zenith angle. Aircraft and lightning NO_x are emitted using a full three-dimensional emission grid. Stratospheric ozone and nitric acid are

Table I
Model emissions in Tg yr^{-1} [a]

Species	Industrial	Biomass burning	Vegetation	Soil	Oceans	Aircraft	Lightning	Other [b]
NO_x	26.6	7.1		5.6		0.5	5.0	
SO_2	72.8	1.6						8.8
H_2	20.0	20.0		5.0	5.0			
CO	684.0	700.0	150.0		50.0			
CH_4	308.9	15.3						260.0
C_2H_4	8.0	7.1	20.0					
C_2H_6	7.0	3.6	3.5					
C_3H_6	10.9	8.2	20.0					
C_3H_8	7.3	1.0	3.5		0.5			
C_4H_{10}	63.1	2.1	8.0					
C_5H_8			500.0					
C_8H_{10}	9.9	1.1						
C_7H_8	9.8							
H_2CO	1.6	1.3						
CH_3CHO	3.5	4.0						
Acetone [c]	2.9	0.5	25.8					
DMS					26.1			
NH_3	39.3	3.5		2.4	8.1			

[a] Emissions are in Tg yr^{-1} except for NO_x which are in Tg N yr^{-1}.
[b] Other methane emissions include rice paddies, tundra, wetlands, termites and animals, both wild and domesticated. Other SO_2 emissions include volcanoes.
[c] Acetone source from vegetation represents production from terpene oxidation.
[d] Emission totals and their spatial distributions were based on entries in the EDGAR database (Olivier et al., 1996).
[e] Aircraft NO_x emissions for 1992 were taken from IPCC (1999).
[f] Vegetation emissions taken from GEIA (Guenther et al., 1995).

treated as emissions into the top model layer using a two-dimensional distribution in the layer between 100 and 200 hPa. Species are removed from the model by dry deposition for air parcels within the boundary layer using species-dependent dry deposition velocities. Nitric acid, hydrogen peroxide, SO_2, sulphate aerosol, nitrate aerosol, N_2O_5 and ammonia are removed by wet scavenging using scavenging factors from Penner et al. (1991).

There are 70 chemical species in the model, including the main trace gas species that are thought to influence the tropospheric ozone and methane budgets: CH_4, CO, NO_x, O_3, hydrogen and nine non-methane organic compounds. A wide range of free radical species have been incorporated into the model in addition to OH and HO_2, the main free radicals involved in the fast photochemistry of the troposphere.

Reaction rate coefficient data and reaction pathways were taken from published reviews and evaluations (Atkinson et al., 1996; DeMore et al., 1997; Atkinson, 2000). These radicals include the organic alkyl peroxy, peroxyacyl, hydroxyperoxy and hexadienylperoxy produced from OH oxidation of alkanes, carbonyl, olefinic and aromatic compounds, respectively. The model species are produced and removed in chemical reactions that are pressure, temperature and time-of-day dependent. Photolysis rates are calculated using a one-dimensional two-stream algorithm (Hough, 1988), taking into account the surface albedo, the overhead ozone column and the instantaneous cloud amount. Altogether the chemical mechanism includes 160 chemical reactions (Collins et al., 1999). The concentration of each species is calculated with a backwards-Euler integration with a chemical timestep of 5 minutes.

The STOCHEM model simulations of ozone and NO_x in the base case experiment have been validated previously against observations in the work of Collins et al. (1997). Results from the present model for CO and O_3 show reasonable agreement with other models and with observations, as can be seen in the intercomparison studies of Kanikadou et al. (1999a,b). A detailed comparison of the STOCHEM model results for the HO_x species with observations is given in Collins et al. (1999). An analysis of the ozone budgets for STOCHEM and 15 other published models is given in Collins et al. (2000).

The oxidising capacity of the troposphere is not always a well-defined quantity, as pollutants are not spread evenly throughout the troposphere but tend to increase in concentration close to sources. As each pollutant has a different global distribution, each pollutant will experience a different oxidising capacity. We have chosen the reaction flux through the methane + OH reaction as our standard measure of the oxidising capacity of the troposphere as methane is the longest lived of the simple organic compounds in the STOCHEM model. In the base case model experiment, the flux through the methane + OH reaction averaged over the 51 months was 500 ± 48 Tg yr^{-1} in good agreement with the IPCC assessment of 490 ± 85 Tg yr^{-1} (IPCC, 1996). This would indicate a methane turnover time due to OH-oxidation of 9.0 ± 0.9 years, in agreement with the IPCC assessment of 9.9 ± 1.8 years (IPCC, 1996).

3. Description of the Model Experiments

The STOCHEM model experiments each began with the meteorological archives on 1 October 1994 and were run forward over the next 51 months until 31 December 1998, with the first three months used for initialisation. Each experiment began on 1 January 1995 when the emission of a particular organic compound was increased for one month and then returned to its base case value. The subsequent transient behaviour of the global troposphere was then followed for four years. The magnitude of the pulse in emissions was arbitrary. It was large enough to generate

measurable differences between the experiment and the base case but small enough to keep the differences in the linear range.

Linearity between the perturbations in trace gas concentrations and the magnitude of the emission pulse was checked using a global 2-D model that has been described elsewhere (Johnson and Derwent, 1996).

Because of the requirements of computer time for our 3-D CTM, we have been unable to complete an exhaustive investigation of the many combinations of spatial patterns for the emission pulses and time of year over which they have been released. Previous work on NO_x (Derwent et al., 2001) has shown that these factors are likely to be important in determining the overall results. In this study we have been restricted to the assessment of the impacts of emission pulses of a wide range of organic compounds using only two spatial distributions for a January emission pulse. Further work will be required to explore a wider range of conditions.

The two spatial distributions used for the additional emission pulses were as follows:

- 'Anthropogenic': for ethane, propane, butane, ethylene, propylene and toluene.
- 'Natural': for methanol, acetaldehyde, acetone and isoprene.

The spatial distributions used for the 'anthropogenic' emission pulses were scaled directly from the global inventories of each organic compound (Olivier et al., 1996), using only those source categories which were driven by human activities (transport, electricity generation etc.). The 'anthropogenic' emission pulses were therefore spread over the major populated and industrialised regions of the world and were almost entirely land-based. The spatial distributions used for the 'natural' emission pulses were the same as that used for the natural biogenic emissions from vegetation appropriate to January and were taken from Guenther et al. (1995). These distributions were largely tropical and were completely land-based. All emission pulses were injected entirely into the model surface layer and only during January 1995.

4. Influence of Ethane on the Oxidising Capacity of the Troposphere

Each organic compound was studied in a separate model experiment that differed only by having an additional emission of that compound during January 1995. In all other respects, the model experiments were identical. To illustrate the results, the model experiment with ethane is described in some detail to set the scene for the other organic compounds whose behaviour was, in principle, exactly analogous to that of ethane.

Figure 1 illustrates the form of the present study. In Figure 1a, the difference in ethane (C_2H_6) emissions between the perturbation and base case experiments is shown. Each column in the plot shows the mean value of that quantity averaged over each month of the model experiment. An extra 1.0 Tg month^{-1} was injected

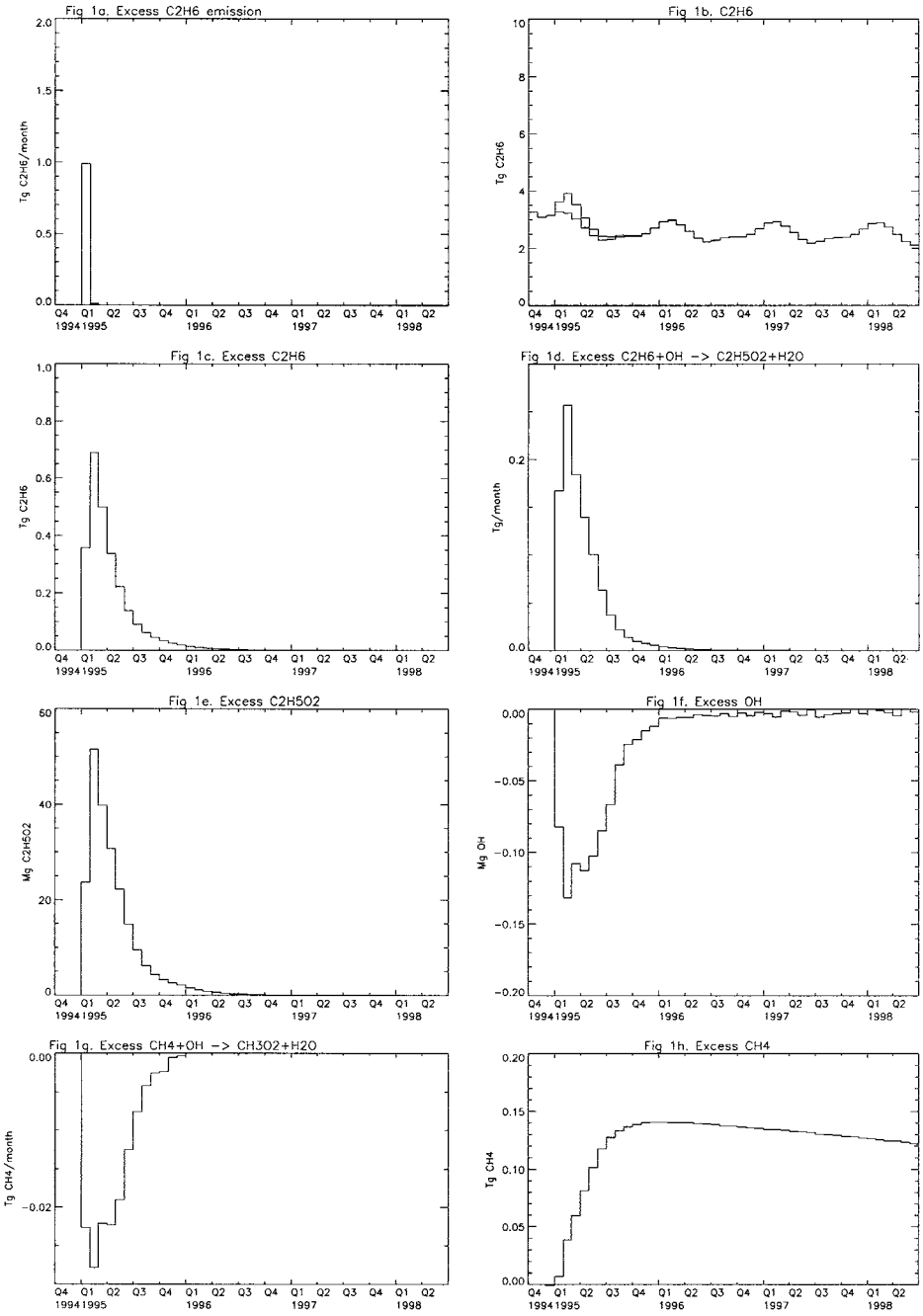

Figure 1. Time development of the perturbed global fluxes and burdens following the addition of an emission pulse of ethane in the 3-D CTM, showing (a) excess C_2H_6 emission, (b) C_2H_6 burdens, (c) excess C_2H_6 burden, (d) excess OH + C_2H_6 flux, (e) excess $C_2H_5O_2$ burden, (f) excess OH burden, (g) excess CH_4 + OH flux, (h) excess CH_4 burden.

over and above the 1.0 Tg month^{-1} in the base case experiment and this is shown in Figure 1a as an 'excess' emission. As a result of the 'excess' emission, the global ethane burdens diverged between the two model experiments, see Figure 1b. By subtracting the results for the two experiments, Figure 1c presents the 'excess' ethane burden.

The monthly mean 'excess' C_2H_6 burden rose from 0.36 Tg during January 1995 and reached a peak of 0.69 Tg during February, before decaying away with an e-folding time of 2.5 months due to oxidation by hydroxyl OH radicals. This time constant is close to the turnover time of C_2H_6 in the base model experiment. Although an extra 1.0 Tg of ethane had been injected, because of its reactivity with OH, the peak 'excess' burden was about two-thirds ($= \exp - {}^1/_{2.5}$) of the 'excess' injection, see Figures 1a–c. The 'excess' C_2H_6 decayed due to the reaction (9):

$$OH + C_2H_6 = C_2H_5O_2 \tag{9}$$

and Figure 1d presents the 'excess' OH + C_2H_6 reaction flux. This enhanced reaction flux, then in turn, generates an 'excess' $C_2H_5O_2$ concentration, see Figure 1e.

The fate of the additional ethylperoxy ($C_2H_5O_2$) radicals depends on the local availability of nitric oxide (NO) and is illustrated in Figure 2. If sufficient NO is available ('high NO_x' conditions) then a rapid reaction sequence follows leading to the recycling of the OH radicals:

$$C_2H_5O_2 + NO = NO_2 + C_2H_5O \tag{10}$$

$$C_2H_5O + O_2 = HO_2 + CH_3CHO \tag{11}$$

$$HO_2 + NO = NO_2 + OH\,. \tag{12}$$

If insufficient NO is available ('low NO_x' conditions) then the $C_2H_5O_2$ will react with HO_2 to form the relatively unreactive ethylhydroperoxide, see Figure 2, with the loss of the free radical species:

$$C_2H_5O_2 + HO_2 = C_2H_5OOH + O_2\,. \tag{13}$$

Overall, Figure 1f shows that the additional flux through the OH + C_2H_6 reaction leads to a 'depletion' in the global OH burden. The peak OH 'depletion' was reached 1–3 months after the emission pulse and decayed rapidly during the first year. The 'depletion' in OH did not go to zero in the same way as the 'excess' C_2H_6 concentrations, C_2H_6 + OH reaction fluxes and $C_2H_5O_2$ concentrations in Figures 1c–e, respectively. A small but significant OH 'depletion' persists throughout the second, third and fourth years of the model experiment when most of responses to the ethane pulse had decayed away.

The OH burden, see Figure 1f, is depleted in the perturbation experiment relative to the base case and this leads to a reduction in the rate of CH_4 oxidation through the OH + CH_4 reaction in reaction (14):

$$OH + CH_4 = CH_3O_2\,. \tag{14}$$

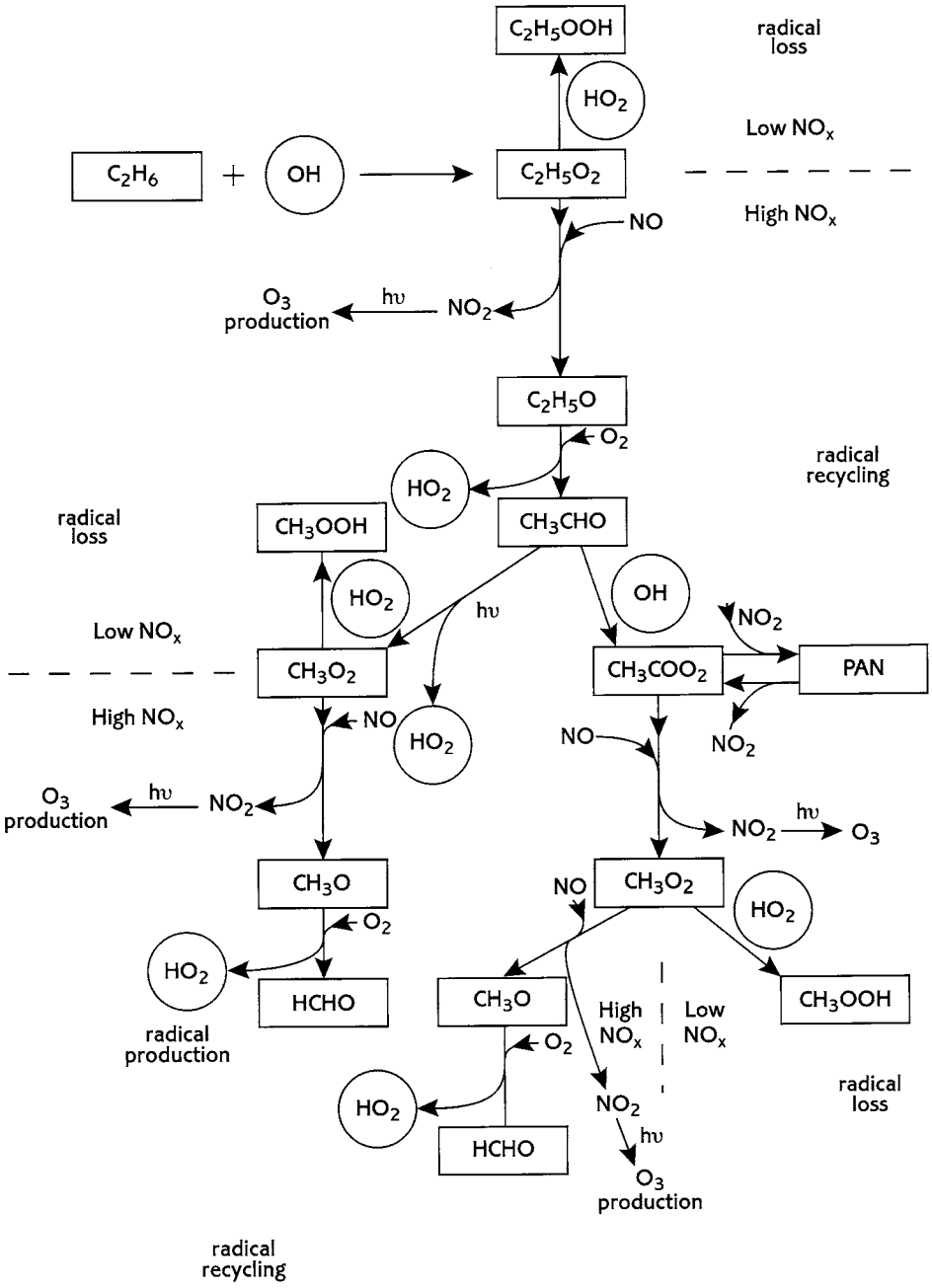

Figure 2. Diagrammatic representation of the atmospheric oxidation pathways for ethane, illustrating the production of ozone, the radical recycling and the radical loss processes under 'high NO_x' and 'low NO_x' conditions.

This reduction in the OH + CH_4 reaction flux is plotted in Figure 1g and leads directly to the build-up of CH_4, relative to the base case. The effect of the additional 1 Tg emission pulse of C_2H_6 has been to produce a perturbation in the fast photochemistry, a depletion in the oxidising capacity of the troposphere and the build-up of a 0.14 Tg 'excess' of CH_4, eleven months later. By the end of the first year of the experiment, all trace of the 'excess' C_2H_6 had decayed away. However, a substantial perturbation in the CH_4 burden remained and as Figure 1h shows, this 'excess' CH_4 decayed slowly over the remaining three years of the experiment. The e-folding time of the 'excess' CH_4 was found to be between 12 and 15 years, which is significantly longer than the CH_4 turnover time of 9.0 ± 0.9 years found in the base case experiment. This difference between the e-folding time and turnover time for methane has been discussed in some detail by Prather (1994). The decay of the 'excess' CH_4 is slower because the additional methane itself reduced the OH concentrations in the perturbation experiment. This 'depletion' in OH is caused by the inefficient recycling of the methylperoxy (CH_3O_2) radicals back to OH since not all of the CH_3O_2 reacts with NO in reaction (17) because some reacts with HO_2 in reaction (18):

$$CH_3O_2 + NO = NO_2 + CH_3O \tag{15}$$

$$CH_3O + O_2 = HO_2 + HCHO \tag{16}$$

$$HO_2 + NO = NO_2 + OH \tag{17}$$

$$CH_3O_2 + HO_2 = CH_3OOH + O_2\,. \tag{18}$$

Hence the 'depletion' in the OH burden (Figure 1f), persists throughout the final three years of the experiment and declines in parallel with the 'excess' CH_4, see Figure 1h.

Figure 3 presents the time development of the impact of the C_2H_6 emission pulse on some of the components of the fast photochemistry. Figure 3a illustrates the formation of 'excess' ozone, formaldehyde (HCHO), Figure 3b, CO, Figure 3c, peroxyacetylnitrate (PAN), Figure 3d. The e-folding decay times of these 'excess' burdens and those of the 'excess' OH + C_2H_6 reaction flux, the $C_2H_5O_2$ and OH burdens were about 2–5 months showing how the time profile of the pulse has been broadened as the chemical perturbation spreads through the fast photochemistry.

5. Emission Pulses of a Range of Simple Organic Compounds

The detailed analysis reported above of the ethane experiment points to two main potential impacts of the emissions of simple organic compounds and their subsequent atmospheric oxidation, on the oxidising capacity of the troposphere:

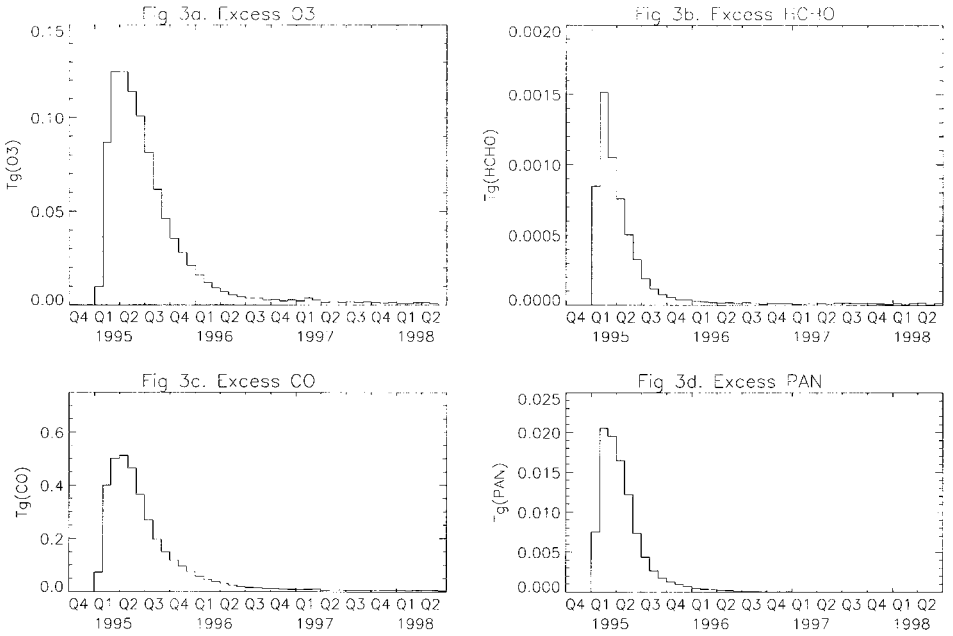

Figure 3. Time development of the perturbed global burdens following the addition of an emission pulse of ethane in the 3-D CTM, showing global excesses of (a) O_3, (b) HCHO, (c) CO, and (d) PAN.

- the rapid production of an ozone perturbation during the first month or so which then decays with an e-folding time of several months,
- the production of a methane perturbation which forms over the period of several months and then decays with an e-folding time of 12–15 years or so, beyond the time frame of the 3-D CTM model experiments.

5.1. PULSE BEHAVIOUR OF ORGANIC COMPOUNDS EMITTED BY HUMAN ACTIVITIES

Figure 4 shows the ozone responses to the addition of an emission pulse of each of the simple organic compounds studied, of which: ethane, propane, butane, ethylene, propylene and toluene were emitted using the 'anthropogenic' spatial distribution. All responses exhibited enhanced ozone production with the rapid generation of a peak excess ozone burden of between 0.05 and 0.6 Tg when each response was normalised to a 1 Tg emission pulse for each organic compound. The 'excess' ozone burdens decayed rapidly, leaving small but indistinct traces after the second year of the experiments. Propylene produced the largest peak 'excess' ozone burden of all of the organic compounds studied and propane the least.

Table II compares the ozone responses from the different organic compounds from human activities injected using the 'anthropogenic' source distribution. The ozone responses have been quantified using the peak excess ozone burdens found

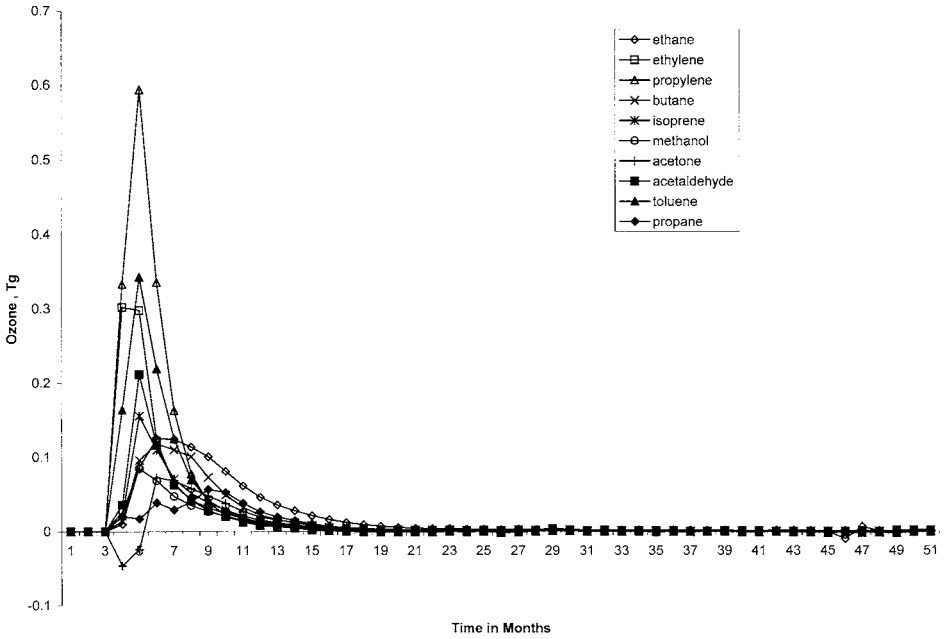

Figure 4. Time development of the excess ozone burden following the addition of an emission pulse of 1 Tg of each organic compound.

Table II

Peak ozone and methane responses to the addition of emission pulses of a range of organic compounds using the 'anthropogenic' source distribution, expressed on a molar basis

Organic compound	Magnitude of emission pulse, Tg	Peak ozone response, Tg per Tg mole injected	Peak methane response, Tg per Tg mole injected
Ethane C_2H_6	30	3.74	4.22
Propane C_3H_8	44	2.50	5.26
Butane C_4H_{10}	58	6.85	5.80
Ethylene C_2H_4	28	8.45	1.71
Propylene C_3H_6	42	24.9	–4.25
Toluene C_7H_8	92	31.5	0.90
CO	28	0.63	1.29

[a] All responses have been converted to a molar basis from a 1 Tg basis by multiplying by the appropriate molecular mass.
[b] The CO responses have been taken from Derwent et al. (2001).
[c] The additional organic compound has been distributed spatially according to the 'anthropogenic' source distribution.

during each experiment and normalising them to a 1 Tmole emission pulse. Peak excess ozone burdens varied between 2.5 and 31.5 Tg on a molar basis, with propane giving the smallest and toluene the largest. All of the organic compounds produced a much larger ozone response compared with carbon monoxide when expressed on a molar basis. This reflects the much larger number of peroxy radical-driven NO to NO_2 interconversions which can follow from the oxidation of one mole of each organic compound compared with that from the oxidation of CO. Each peroxy radical-driven NO to NO_2 interconversion may produce an additional ozone molecule through the reaction sequence:

$$RO_2 + NO = RO + NO_2 \tag{19}$$

$$NO_2 + h\nu = NO + O \tag{4}$$

$$O + O_2 + M = O_3 + M\,. \tag{5}$$

A number of factors influenced the peak ozone responses from each of the organic compounds in Table II. OH reactivity increases along the series: ethane<propane< butane and ethylene<propylene and ethane<ethylene<toluene. The more reactive compounds are oxidised closer to the source regions under 'high NO_x' conditions and hence produce more ozone from $RO_2 + NO$ reactions whereas the less reactive compounds are oxidised under 'low NO_x' conditions and lead to more peroxy radical loss through $RO_2 + HO_2$ reactions. The peak ozone responses build up quickly with the complexity of the organic compounds studied since increasing molecular complexity tends to increase both OH reactivity and the potential number of peroxy radical-driven NO to NO_2 interconversions following the complete oxidation of the organic compound. The one exception appears to be propane, see Table II, whose peak ozone response is out of step with those of ethane and butane. This is because of the formation of acetone as a major reaction product in the oxidation of propane. Acetone has an unusually long lifetime for a carbonyl compound compared with the corresponding lifetimes of the carbonyl reaction products of ethane and butane oxidation. Hence much of the oxidation of acetone occurs far removed from the point of emission of the propane and necessarily under 'low NO_x' conditions.

Figure 5 illustrates the methane responses that were found following the addition of an emission pulse of each of the simple organic compounds studied. The different peak methane responses to the emission pulses of each organic compound are also compared quantitatively in Table II on a molar basis. If the oxidation of each organic compound had merely converted one OH radical into an HO_2 radical, then the peak methane responses for each organic compound should be similar to that of CO on a molar basis. That this is not the case implies that there must be an important role for the peroxy radicals formed from the oxidation of each organic compound in determining the sources and sinks of the HO_x radical species.

Ethane, propane and butane show peak methane responses on a molar basis which are 3–5 times greater than that of CO, pointing to their large influence on

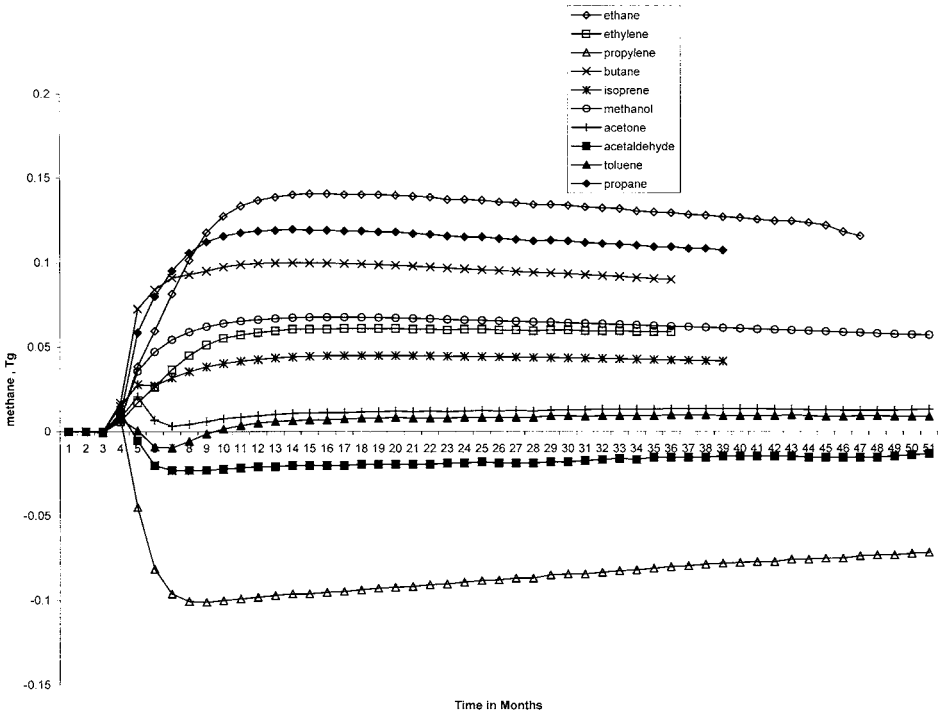

Figure 5. Time development of the excess methane burden following the addition of an emission pulse of 1 Tg of each organic compound.

the sources and sinks of the HO_x radicals which arises because of their generally low reactivity. This low reactivity means that a significant fraction of the additional emission pulse appears to have been oxidised well away from the point of emission under 'low NO_x' conditions. This leads to enhanced radical loss through $RO_2 + HO_2$ reactions and increased peak methane responses. Increasing molecular complexity increases the potential number of $RO_2 + HO_2$ peroxy radical loss processes but increases reactivity and hence decreases the fraction of the additional emission pulse oxidised under 'low NO_x' conditions.

Ethylene and toluene are both reactive organic compounds which are largely oxidised under 'high NO_x' conditions leading to enhanced ozone production. Furthermore, ethylene and toluene oxidation leads to the production of photochemically labile aldehydes that can enhance peroxy radical production enough to offset peroxy radical loss. Hence peak methane responses on a molar basis for ethylene and toluene are only slightly higher than that of CO despite their increased molecular complexity.

The peak methane response following the emission pulse of propylene was negative, see Table II, whereas the corresponding values for all of the other entries in the Table were positive. The oxidation of the additional pulse of propylene

generated a significant amount of excess peroxyacetyl nitrate through reactions (22–26):

$$OH + C_3H_6 + O_2 = OHC_3H_6O_2 + H_2O \quad (19)$$

$$OHC_3H_6O_2 + NO = NO_2 + OHC_3H_6O \quad (20)$$

$$OHC_3H_6O + O_2 = HO_2 + CH_3CHO + HCHO \quad (21)$$

$$OH + CH_3CHO + O_2 = CH_3COO_2 + H_2O \quad (22)$$

$$CH_3COO_2 + NO_2 + M = PAN + M\,. \quad (23)$$

An 'excess' of about 0.1 Tg PAN built up quickly following the propylene emission pulse and this transported additional NO_y away from the source regions. This PAN subsequently decomposed, liberating NO_x which then led to increased OH concentrations and enhanced methane oxidation, through the reaction sequence:

$$PAN + M = CH_3COO_2 + NO_2 \quad (24)$$

$$NO_2 + h\nu = NO + O \quad (4)$$

$$O + O_2 + M = O_3 + M \quad (5)$$

$$NO + HO_2 = OH + NO_2\,. \quad (17)$$

No other organic compound in Table II exhibited the enhanced production of PAN to the same extent as propylene.

5.2. PULSE BEHAVIOUR OF ORGANIC COMPOUNDS EMITTED BY VEGETATION

Figure 4 shows the ozone responses to the addition of the emission pulses of methanol, acetaldehyde, acetone and isoprene using the 'vegetation' spatial distribution to represent natural biogenic sources. Whereas the emission pulses of methanol, acetaldehyde and isoprene generated analogous ozone responses to those produced by the organic compounds emitted with the 'anthropogenic' spatial distribution, acetone showed a distinctly different behaviour during the first few months. The ozone response first showed an ozone 'depletion' that later changed sign to become an 'excess', before decaying away in an analogous manner to the other ozone responses.

Figure 5 shows the corresponding methane responses to the addition of methanol, acetaldehyde, acetone and isoprene using the 'vegetation' spatial distribution. Whereas the methane responses to the organic compounds emitted with the 'anthropogenic' spatial distribution were all relatively simple, only that of methanol followed the same simple response. Acetaldehyde produced a methane

response that changed sign from an 'excess' to a 'depletion' before decaying away. Acetone and isoprene showed large initial methane responses that subsequently decreased dramatically before decaying away more slowly.

An important consideration in understanding the ozone and methane responses to the emission pulses of the organic compounds emitted with the 'vegetation' distribution is that they do not overlay as effectively with the source distribution of NO_x as with the 'anthropogenic' distribution. As a consequence, it is anticipated that the organic compounds emitted with the 'vegetation' distribution are more likely to be oxidised in 'NO_x limited' regions compared with those with the 'anthropogenic' distribution. All other things being equal, this should lead to decreased ozone responses and increased methane responses.

The addition of the acetaldehyde pulse leads to an increased flux through the OH + CH_3CHO reaction during January, increased peroxy radical concentrations, increased PAN levels, decreased NO_x and decreased O_3 levels throughout the 'NO_x limited' 'vegetation' source region. Outside of this region, increased PAN vertical convective transport led to increased NO_x levels in the remote mid and upper troposphere and hence increased ozone levels. The extra O_3 in these remote regions more than compensated for the loss of NO_x in the source regions and so, overall, an ozone 'excess' appeared. Hydroxyl concentrations decreased due to increased OH + CH_3CHO oxidation and so a methane 'excess' built up close to the acetaldehyde source.

During February, the acetaldehyde pulse decayed away quickly, the PAN reverted to NO_x and so stimulated ozone and OH production. This additional OH production from ozone photolysis, increased the flux through the OH + CH_4 reaction and led to the production of a methane 'depletion'. This caused the change in sign of the methane response found with acetaldehyde in Figure 5.

Because acetone is much less reactive compared to acetaldehyde, its ozone and methane responses are quite different despite the similarities in their atmospheric oxidation pathways. During January, the additional acetone photolyses in the mid and upper troposphere produced additional peroxy radicals. However, OH oxidation led to the formation of PAN and the depletion of NO_x. Ozone and OH levels therefore decreased in the upper troposphere because of the decreased availability of NO_x. Additional PAN was transported to the surface and led to increased NO_x levels, increased ozone and increased OH. However, upper tropospheric changes masked surface changes and so overall, ozone and OH decreased and methane increased during January.

Because of the longer lifetime of acetone compared to that of acetaldehyde, the initial responses persist longer into the experiment. However, by March, much of the acetone pulse has decayed away and with it the PAN and OH responses. Ozone levels remained higher than in the base case experiment because of the presence of 'excess CO' and the increased ozone production through the HO_2 + NO reaction that it stimulated. Hence, a small ozone 'excess' built up, reversing the initial ozone 'depletion'. This 'excess' ozone is associated with a small 'excess'

Table III

Peak ozone and methane responses to the addition of emission pulses of a range of organic compounds using the 'vegetation' source distribution, expressed on a molar basis

Organic compound	Magnitude of emission pulse, Tg	Peak ozone response, Tg per Tg mole injected	Peak methane response, Tg per Tg mole injected
Isoprene C_5H_8	68	9.34	2.70
Methanol CH_3OH	32	2.70	2.17
Acetaldehyde CH_3CHO	44	9.33	–1.01
Acetone CH_3COCH_3	58	4.19	0.78

[a] All responses have been converted to a molar basis from a 1Tg basis by multiplying by the appropriate molecular mass.
[b] The additional organic compound has been distributed spatially according to the source distribution for 'vegetation' during January.

methane, caused largely by an increased flux through the OH + CO reaction which led to a decrease in the flux through the OH + CH_4 reaction.

Table III compares the ozone responses from the different organic compounds from vegetation injected using the 'natural' source distribution. The ozone responses have been quantified using the peak excess ozone burdens found during each experiment and normalising them to a 1 Tmole emission pulse. Peak excess ozone burdens varied between 2.7 and 9.3 Tg on a molar basis, with methanol giving the smallest value and isoprene the largest. All of the organic compounds produced a much larger ozone response compared with carbon monoxide when expressed on a molar basis, reflecting the much larger number of peroxy radical-driven NO to NO_2 interconversions per mole of compound oxidised compared with CO.

Reactivity with OH is not such an issue for the 'natural' compounds as it is with the 'anthropogenic' compounds as can be seen from the narrower range in ozone responses between acetone and isoprene in Table III compared with that between propane and toluene in Table II. Acetone and isoprene have lifetimes that differ by orders of magnitude yet they show little difference in peak ozone responses. Because of the 'low NO_x' conditions, ozone responses are much reduced below those found in Table II for 'high NO_x' conditions and exhibit a much reduced dependence on reactivity.

The structural complexity of the organic compounds makes a significant difference to the ozone responses in that the more complex the molecular structure of the organic compound the more peroxy radical-driven NO to NO_2 interconversions should result during its atmospheric oxidation. Although there is some evidence that peak ozone responses increase with molecular complexity across Table III, its

influence is not dominating. The factor which best explains the increasing peak ozone responses: methanol < acetone < acetaldehyde = isoprene appears to be the detailed atmospheric degradation pathways of the organic compounds involved and the behaviour of the intermediate compounds formed, particularly PAN. Methanol is the simplest organic compound in Table III. It lacks any ability to form PAN and exhibits only one peroxy radical-driven NO to NO_2 interconversion in its oxidation pathway, through reactions (26) and (27):

$$OH + CH_3OH + O_2 = O_2CH_2OH + H_2O \tag{26}$$

$$O_2CH_2OH + NO = NO_2 + HO_2 + HCHO\,. \tag{27}$$

In contrast, acetaldehyde may react with OH radicals in reactions (23) and (24) to generate PAN or it may photolyse generating further free radicals. Further peroxy radical-driven NO to NO_2 interconversion will result in either case, increasing its peak ozone response above that exhibited by methanol. The important role of PAN in locking up NO_x in the source regions has been described above. Acetone contains more C–H and C–C bonds compared with acetaldehyde and should show enhanced ozone productivity. However, because of its long lifetime of acetone, the role played by PAN was distinctly different in that it locked up NO_x in the more remote regions of the troposphere. Isoprene should exhibit by far the largest ozone productivity but its potential is limited because it reacts largely under 'NO_x limited' conditions close to the source regions.

The peak methane responses in Table III from the 'natural' organic compounds should be greater than those of the 'anthropogenic' compounds in Table III because the former are oxidised under 'low-NO_x' conditions which should favour peroxy radical loss through RO_2 + HO_2 reactions and hence loss of OH. However, the main influence appears to be the detailed atmospheric reaction pathways and the behaviour of the intermediate species formed, such as PAN. With acetaldehyde, the methane 'depletion' is caused by the decay of the 'excess' PAN which had been transported to the mid and upper troposphere. With acetone, the methane 'excess' is caused by the oxidation of acetone in the mid and upper troposphere which forms 'excess' PAN and reduces both NO_x and OH.

6. Indirect Global Warming Potentials for each Organic Compound

Here, we define the Global Warming Potentials GWP of an organic compound as the ratio of the time-integrated radiative forcing for a particular radiative forcing mechanism resulting from the emission of a pulse of 1 Tg of that compound compared with that from the emission of 1 Tg (as CO_2) of CO_2 over a hundred year time horizon. There are two steps therefore in assessing the indirect global warming potential of an organic compound. In the first step, the time-integrated 'excess' burdens (or depletions) in methane and ozone must be estimated over a

Table IV

Time-integrated excess methane and ozone burdens following the emission of a pulse of an organic compound, normalised to 1 Tg of each compound, and their radiative forcings, over a 100-year time horizon

Organic compound	Time-integrated 'excess' CH_4, Tg years	Time-integrated 'excess' O_3, Tg years	Time-integrated CH_4 radiative forcing, m W m^{-2} years	Time-integrated O_3 radiative forcing, m W m^{-2} years
'Anthropogenic' compounds on a 1 Tg emitted basis				
Ethane	1.77	0.077	0.30	0.28
Propane	1.60	0.035	0.29	0.06
Butane	1.44	0.057	0.25	0.17
Ethylene	0.93	0.081	0.16	0.23
Propylene	–1.22	0.132	–0.21	0.40
Toluene	0.14	0.088	0.02	0.27
'Natural' compounds on a 1 Tg emitted basis				
Isoprene	0.65	0.047	0.11	0.17
Methanol	0.95	0.032	0.16	0.12
Acetaldehyde	0.23	0.047	–0.04	0.18
Acetone	0.21	0.027	0.04	0.02

100-year time horizon for a 1 Tg pulse of each compound. In the second step, these time-integrated burdens must be converted into radiative forcings. The first step is straightforward for ozone since the 'excess' burdens had largely decayed away during the four-year experiments. The time-integrated ozone burdens in Table IV over the 4 years experiments are therefore identical to the required burdens over the 100-year time horizon. For methane, the 'excess' burdens had not decayed away at the end of the 4 years experiments with any of the organic compounds studied and so the time-integrated 'excess' methane burdens over a hundred year time horizon were obtained integrating the methane excesses up to the end of the 4th year and adding on a contribution covering the fifth and subsequent years. This contribution was estimated using the 'excess' methane burden during December 1998, B_f, and the e-folding time of its decay in years, T, as follows:

$$\text{Time-integrated excess} = \text{integrated excess for the first 4 years} + B_f T \,,$$

where T was taken to be 12.2 years (Derwent et al., 2001). The time-integrated methane and ozone burdens over the 100-year time horizon following the addition of a Tg emission pulse of each organic compound have been tabulated in Table IV.

To complete the second step in the assessment of indirect global warming potentials, we have used the radiative forcing formulae for methane laid out by IPCC (1990) and converted the time-integrated excess methane concentrations into time-integrated radiative forcing, over a 100 year time horizon. On this basis, for example, a 1 Tg emission pulse of ethane produced a time-integrated excess methane burden of 1.77 Tg years and a time-integrated radiative forcing of 0.3 mW m^{-2} year over a 100 year time horizon, see Table IV.

To estimate the radiative forcing consequences of the tropospheric ozone changes found in the 3-D CTM we employed the Edwards and Slingo (1996) radiation code at low spectral resolution. Clouds and temperatures were represented using the meteorological archives driving the 3-D CTM. Stratospheric temperatures were iteratively adjusted until stratospheric heating rates returned to their unperturbed values and details of the methodology are given elsewhere (Stevenson et al., 1998). Estimates of ozone radiative forcing due to changes in tropospheric ozone since pre-industrial times agree closely with other published estimates (Berntsen et al., 1997; Haywood et al., 1998; Kiehl et al., 1999). The radiative forcing caused by the differences between the transient and base cases were calculated for each month of the first year of each perturbation experiment. This radiative forcing was proportional to the ozone response with a linearity factor of 0.023 W m^{-2} per ppb change in the global mean ozone concentration in the 4.8–11.2 km, 500–200 mb altitude range or 0.003 W m^{-2} per Tg change in the global tropospheric ozone burden. In estimating the time-integrated ozone radiative forcing in Table IV, it was assumed that radiative forcing was linear in ozone burden change in the second and subsequent years of each perturbation experiment. On this basis, a 1 Tg emission pulse of ethane produced a time-integrated ozone radiative forcing of 0.28 mW m^{-2} years over a 100 year time horizon.

The organic compounds that are derived from fossil-carbon will ultimately generate additional carbon dioxide as they degrade in the atmosphere. The fate of this CO_2 was described using the CO_2 response function of the Bern carbon cycle model (IPCC, 1996) run for a constant mixing ratio of CO_2 over a 500-year period.

The time-integrated radiative forcing estimates for the different forcing mechanisms and for the different tropospheric ozone precursors have been converted into global warming potentials (GWPs) by comparison with the time-integrated forcing of a reference gas, taken to be CO_2. The resulting indirect GWPs are presented in Table V. They are presented here, not as definitive estimates for use by policy-makers, but to demonstrate that the emissions of organic compounds have potentially important indirect radiative impacts upon the distributions of methane and ozone. Hence, GWPs for the 100-year time horizon suffice at this preliminary stage in their assessment.

The tabulated GWPs have some significant inherent uncertainties which arise from uncertainties in the representation in the model of the oxidation of the individual organic compounds and the methane and ozone responses, from the calculation of the methane and ozone radiative forcings and that of the reference gas, CO_2

Table V

Indirect global warming potentials for each organic compound for each radiative forcing mechanism involving methane, ozone and carbon dioxide

Organic compound	GWP^{CH_4}	GWP^{O_3}	GWP^{CO_2}
'Anthropogenic' compounds on a 1 Tg emitted basis			
Ethane	2.9	2.6	2.9
Propane	2.7	0.6	3.0
Butane	2.3	1.7	3.0
Ethylene	1.5	2.2	3.1
Propylene	–2.0	3.8	3.1
Toluene	0.2	2.5	3.3
'Natural' compounds on a 1 Tg emitted basis			
Isoprene	1.1	1.6	
Methanol	1.6	1.2	
Acetaldehyde	–0.4	1.7	
Acetone	0.3	0.2	

[a] The corresponding GWP^{CH_4}, GWP^{O_3} and GWP^{CO_2} values for CO are 1.0 ; 0.5 ; 1.6.
[b] The GWP^{CO_2} values for 'natural' emissions are by definition identically zero.
[c] Uncertainty ranges are estimated to be from –50% to +100% about the central values, see text, that is, encompassing a factor of four.

which underpins the GWP concept. The uncertainties in the GWPs for well-mixed gases are given as ±35% (IPCC, 1996) and so, accordingly, we have estimated a wider uncertainty range of –50% to +100% about the central value for the organic compounds in Table V.

7. Discussion and Conclusions

In this study, we have shown that the addition of an emission pulse of a range of organic compounds into the troposphere, induces transient responses in the global 3-D distributions of methane and ozone, two of the more important radiatively-active trace gases. Following on quickly from the emission pulse, a sharp rise in ozone concentrations was observed which then decayed with an e-folding time of several months. A rise (or fall) in methane concentrations then formed steadily over the period of months and then decayed with an e-folding time of 10 years or so. We have shown that pulses of short-lived organic compounds can induce perturbations in the tropospheric distributions of methane and ozone that are long-

lived and decay on a 10–15 year timescale. In this behaviour, organic compounds appear to behave in exactly the same manner as that previously demonstrated for methane (Prather, 1994, 1996; Wild and Prather, 2000), carbon monoxide (Prather, 1996; Daniel and Solomon, 1998; Wild and Prather, 2000) and NO_x (Wild and Prather, 2000) and hydrogen (Derwent et al., 2001).

The magnitudes of these 'excess' ozone and methane burdens were determined for each organic compound. The radiative forcing consequences of the 'excess' burdens were then estimated and compared with the radiative forcing consequences of the emission of an identical mass of carbon dioxide, evaluated over a 100-year time horizon. The Global Warming Potentials GWPs were then calculated as the ratio of the radiative forcing from methane or ozone relative to that of carbon dioxide.

The GWP^{CH_4}s for the simple organic compounds found in this study covered a range from –2.0 to 2.9 when expressed on a mass basis for each compound over a 100-year time horizon. The corresponding GWP^{CH_4} for CO was 1.0 (Derwent et al., 2001) determined with an identical methodology. Of the 10 simple organic compounds studied, six had GWP^{CH_4}s that were larger than that of CO, two were negative and the remaining two were positive and significantly smaller than that of CO.

In assessing the transient methane responses to the emission pulses of the different organic compounds, the following crucial factors emerged:

- *spatial distribution* of the emission pulse, whether 'anthropogenic' or 'natural', since this governed whether the organic compound was oxidised under 'high NO_x' or 'low NO_x' conditions, giving low GWP^{CH_4} or high GWP^{CH_4}s, respectively,
- *reactivity*, since again this governed whether the organic compound was oxidised under 'high NO_x' or 'low NO_x' conditions,
- *molecular complexity*, since the greater the number of C–C or C–H bonds in the molecule the more RO_2 + HO_2 reactions could occur, leading to greater GWP^{CH_4}s,
- whether *aldehydes* were formed in the major degradation pathways since through their photolysis they could offset RO_2 loss and lead to lower GWP^{CH_4}s,
- whether *PAN formation* is a major atmospheric pathway, leading to negative GWP^{CH_4}s, as with acetaldehyde and propylene.

The GWP^{O_3}s in Table V for all the organic compounds studied are positive and encompass the range from 0.2 to 3.8. This is a reflection of the importance of organic peroxy radical driven NO to NO_2 conversions as a source of ozone. The less reactive man-made organic compounds tend to be oxidised further away from their sources under 'NO_x limited' conditions giving rise to lower GWP^{O_3}s.

In assessing the transient responses of ozone to the emission pulses of the different organic compounds, the same crucial factors emerged as for the methane

transient responses. These were spatial distribution, reactivity, molecular complexity, formation of aldehydes (as opposed to unreactive carbonyl compounds such as acetone) and PAN formation. As a result, GWP^{O_3}s were larger for the 'anthropogenic' compounds compared with the 'natural' compounds. The GWP^{O_3} value for propane was low because of the importance of the formation of unreactive acetone in its atmospheric oxidation pathway.

As far as we are aware, these are the first reported determinations of the GWPs for organic compounds, other than our own previous studies with a 2-D global CTM (Johnson and Derwent, 1996). It appears that the problems inherent in 2-D models have had a major influence on the responses of methane and ozone to emissions of organic compounds, reinforcing their inadequacy. Many of the shortcomings inherent in previous 2-D CTM studies, as discussed in detail elsewhere (Johnson and Derwent, 1996), have been addressed in this 3-D CTM study.

In the past, the Intergovernmental Panel on Climate Change have deliberately not recommended relative radiative forcing indices, global warming potentials included, for short-lived organic compounds and have only provided estimates for well-mixed greenhouse gases (IPCC, 1996). There are a number of reasons why GWPs for short-lived trace gases have been considered uncertain and unreliable. The first and perhaps most important reason has been the lack of availability of state-of-the-art global 3-D model studies of the influence of short-lived trace gases on the fast photochemistry of the troposphere which controls the global distributions of methane and ozone. The second reason is that the influence of the short-lived trace gases is likely to be inherently more variable in space and time and that these variations would be difficult to express in a single number for a GWP.

Questions still remain concerning the spatial and temporal variations in GWPs for short-lived trace gases and the detailed mechanisms of the atmospheric oxidation reactions of organic compounds. This study has considered only a very limited range of plausible locations and timescales for the emission pulses because of the computational demands of 3-D CTMs. Furthermore, it has addressed only the behaviour during the northern hemisphere winter. Nevertheless, in this initial study, we have shown that organic compounds do indeed have indirect radiative impacts and that these impacts are distinctly different depending on whether the organic compounds are emitted with NO_x from human activities over the mid-latitude continental regions or whether they are emitted in tropical regions from vegetation sources. The different GWPs found here for the organic compounds emitted with different spatial patterns are entirely consistent with current understanding of the importance of tropospheric photochemistry under 'low NO_x' or 'high NO_x' conditions.

On balance, our studies show that GWPs for short-lived organic compounds are likely to be spatially and temporally variable. This study has begun the process of starting to quantify GWPs for them by choosing one northern hemisphere winter month to perform the emission pulse and by using previously published spatial pat-

terns to define the spatial context. The aim is to steadily extend the coverage of the GWPs with further studies as understanding of tropospheric chemistry develops.

In an attempt to consider what clues can be gleaned as to the relative importance for global warming of the emissions of organic compounds from human activities, we have used the GWPs calculated here and multiplied them by the corresponding emissions from Table I. Looking first at the radiative forcing from the well-mixed greenhouse gas, methane, then GWP-weighted emissions appear to be heavily dominated by the emissions of butane. Looking then at the more regional in character radiative forcing from tropospheric ozone, then again, butane emissions appear to be the most crucial. Although methane is considered within the scope of the Framework Convention on Climate Change, this is not the case for the other tropospheric ozone precursors, particularly NO_x and organic compounds. Hansen et al. (2000) have pointed out the importance of non-CO_2 greenhouse gases for policy during the next 50 years. A case can be made for their inclusion in the Framework Convention alongside methane, if future methane and tropospheric ozone levels are to be stabilised and eventually reduced to combat global climate change. However, in view of the dependence of the GWPs presented here on where the ozone precursor gases are released, it is concluded that this study is just the beginning of those needed for a detailed assessment of GWPs for organic compounds. Further work is required to extend the range of organic compounds covered and to explore a wider range of source distributions and seasons.

Acknowledgements

This study was supported as part of the Public Meteorological Service R&D Programme of the Met Office and by the Department of the Environment, Transport and the Regions through contracts PECD 7/12/37 (Global Atmosphere Division) and EPG 1/3/164 (Air and Environmental Quality Division). DS was funded by a NERC UGAMP fellowship.

References

Atkinson, R.: 2000, 'Atmospheric Chemistry VOCs and NO_x', *Atmos. Eviron.* **34**, 2063–2101.

Atkinson, R., Baulch, D. L., Cox, R. A., Hampson, R. F., Kerr, J. A., Rossi, M. J., and Troe, J.: 1996, 'Evaluated Kinetic and Photochemical Data for Atmospheric Chemistry. Supplement V. IUPAC Subcommittee on Gas Kinetic Data Evaluation for Atmospheric Chemistry', *Atmos. Environ.* **30**, 3903–3904.

Berntsen, T. K., Isaksen, I. S. A., Myhre, G., Fuglestvedt, J. S., Stordal, F., Larsen, T. A., Freckleton, R. S., and Shine, K. P.: 1997: 'Effects of Anthropogenic Emissions on Tropospheric Ozone and Its Radiative Forcing', *J. Geophys. Res.* **102**, 28101–28126.

Collins, W. J., Derwent, R. G., Johnson, C. E., and Stevenson, D. S.: 2000, 'The Impact of Human Activities on the Photochemical Production and Destruction of Tropospheric Ozone', *Quart. J. Roy. Meteorol. Soc.* **126**, 1925–1951.

Collins, W. J., Stevenson, D. S., Johnson, C. E., and Derwent, R. G.: 1997, 'Tropospheric Ozone in a Global-Scale Three-Dimensional Lagrangian Model and Its Response to NO_x Emissions Controls', *J. Atmos. Chem.* **26**, 223–274.

Collins, W. J., Stevenson, D. S., Johnson, C. E., and Derwent, R. G.: 1999, 'The Role of Convection in Determining the Budget of Odd Hydrogen in the Upper Troposphere', *J. Geophys. Res.* **104**, 26927–26941.

Cooke, W. F. and Wilson, J. J. N.: 1996, 'A Global Black Carbon Aerosol Model', *J. Geophys. Res.* **101**, 19395–19409.

Crutzen, P. J.: 1974, 'Photochemical Reactions Initiated by and Influencing Ozone in the Unpolluted Troposphere', *Tellus* **26**, 47–57.

Cullen, M. J. P.: 1993: 'The Unified Forecast/Climate Model', *Met. Mag.* **122**, 81–94.

Daniel, J. S. and Solomon, S.: 1998, 'On the Climate Forcing of Carbon Monoxide', *J. Geophys. Res.* **103**, 13249–13260.

Demerjian, K. L., Kerr, J. A., and Calvert, J. G.: 1974, 'Mechanism of Photochemical Smog Formation', *Adv. Environ. Sci. Technol.* **4**, 1–262.

DeMore, W. B., Sander, S. P., Golden, D. M., Hampson, R. F., Kurylo, M. J., Howard, C. J., Ravishankara, A. R., Kolb, C. E., and Molina, M. J.: 1997, *Chemical Kinetics and Photochemical Data for Use in Stratospheric Modeling*, Evaluation Number 12, JPL Publ. 97-4, Jet Propulsion Laboratory, Pasadena, California.

Derwent, R. G.: 1990, *Trace Gases and their Relative Contribution to the Greenhouse Effect*, AERE Report R-13716, H. M. Stationery Office, London.

Derwent, R. G., Collins, W. J., Johnson, C. E., and Stevenson, D. S.: 2001, 'Transient Behaviour of Tropospheric Ozone Precursors in a Global 3-D CTM and their Indirect Greenhouse Effects', *Clim. Change* **49**, 463–487.

Edwards, J. M. and Slingo, A.: 1996, 'Studies with a Flexible New Radiation Code. I: Choosing a Configuration for a Large-Scale Model, *Quart. J. Roy. Meteorol. Soc.* **122**, 689–719.

Ehhalt, D. H.: 1974, 'The Atmospheric Cycle of Methane', *Tellus* **26**, 58–70.

Fuglestvedt, J. S., Berntsen, T., Isaksen, I. S. A., Mao, H., Liang, X. Z., and Wang, W. C.: 1999, 'Climatic Forcing of Nitrogen Oxides through Changes in Tropospheric Ozone and Methane; Global 3-D Model Studies', *Atmos. Environ.* **33**, 961–977.

Guenther, A., Hewitt, C. N., Erickson, D., Fall, R., Geron, C., Graedel, T., Harley, P., Klinger, L., Lerdau, M., McKay, W. A., Pierce, T., Scholes, B., Steinbrecher, R., Tallamraju, R., Taylor, J., and Zimmerman, P.: 1995, 'A Global Model of Natural Volatile Organic Compound Emissions', *J. Geophys. Res.* **100**, 8873–8892.

Haywood, J. M., Schwarzkopf, M. D., and Ramaswamy, V.: 1998, 'Estimates of Radiative Forcing Due to Modeled Increases in Tropospheric Ozone', *J. Geophys. Res.* **103**, 16999–17007.

Hansen, J., Sato, M., Ruedy, R., Lacis, A., and Oinas, V.: 2000, 'Global Warming in the Twenty-First Century: An Alternative Scenario', *Proc. Nat. Acad. Sci.* **97**, 9875–9880.

Hough, A. M.: 1988, *The Calculation of Photolysis Rates for Use in Global Tropospheric Modelling Studies*, UKAEA Harwell Report AERE R 13259, Oxfordshire.

IPCC: 1995, *Radiative Forcing of Climate Change*, The 1994 Report of the Scientific Assessment Working Group of the IPCC, WMO UNEP, Geneva.

IPCC: 1996, *Climate Change 1995: The IPCC Scientific Assessment*, Cambridge University Press, Cambridge.

Isaksen, I. S. A. and Hov, O.: 1987, 'Calculation of Trends in the Tropospheric Concentration of O_3, OH, CO, CH_4 and NO_x', *Tellus B* **33**, 271–285.

Johnson, C. E. and Derwent, R. G.: 1996, 'Relative Radiative Forcing Consequences of Global Emissions of Hydrocarbons, Carbon Monoxide and NO_x from Human Activities Estimated with a Zonally-Averaged Two-Dimensional Model', *Clim. Change* **34**, 439–462.

Kanakidou, M., Dentener, F. J., Brasseur, G. P., Collins, W. J., Berntsen, T. K., Hauglustaine, D. A., Houweling, S., Isaksen, I. S. A., Krol, M., Law, K. S., Lawrence, M. G., Muller, J. F., Plantevin,

P. H., Poisson, N., Roelofs, G. J., Wang, Y., and Wauben, W. M. F.: 1998, *3-D Global Simulations of Tropospheric Chemistry with Focus on Ozone Distributions*, EUR 18842 Report, European Commission, Office for Official Publications of the European Communities, Luxembourg.

Kanikadou, M., Dentener, F. J., Brasseur, G. P., Berntsen, T. K., Collins, W. J., Hauglustaine, D. A., Houweling, S., Isaksen, I. S. A., Krol, M., Lawrence, M. G., Muller, J. F., Poisson, N., Roelofs, G. J., Wang, Y., and Wauben, W. M. F.: 1999, '3-D Global Simulations of Tropospheric CO Distributions – Results of the GIM/IGAC Intercomparison 1997 Exercise', *Chemosphere: Global Change Sci.* **1**, 263–282.

Kheshgi, H. S., Jain, A. K., Kotamarthi, R., and Wuebbles, D. J.: 1999: 'Future Atmospheric Methane Concentrations in the Context of the Stabilisation of Greenhouse Gas Concentrations', *J. Geophys. Res.* **104**, 19183–19190.

Kiehl, J. T., Schneider, T. L., Portmann, R. W., and Solomon, S.: 1999, 'Climate Forcing Due to Tropospheric and Stratospheric Ozone', *J. Geophys. Res.* **104**, 31239–31254.

Lacis, A. A., Wuebbles, D. J., and Logan, J. A.: 1990, 'Radiative Forcing of Climate by Changes in the Vertical Distribution of Ozone', *J. Geophys. Res.* **95**, 9971–9981.

Leighton, P. A.: 1961, *Photochemistry of Air Pollution*, Academic Press, New York.

Levy, H.: 1971, 'Normal Atmosphere: Large Radical and Formaldehyde Concentrations Predicted', *Science* **173**, 141–143.

Murphy, D. M. and Fahey, D. W.: 1994, 'An Estimate of the Flux of Stratospheric Reactive Nitrogen and Ozone into the Troposphere', *J. Geophys. Res.* **99**, 5325–5332.

Olivier, J. G. J., Bouwman, A. F., van der Maas, C. W. M., Berdowski, J. J. M., Veldt, C., Bloos, J. P. J., Visschedijk, A. J. H., Zandveld, P. Y. J., and Haverlag, J. L.: 1996, *Description of EDGAR Version 2.0*, RIVM Report Nr. 771060 002, Bilthoven.

Olson, J., Prather, M., Berntsen, T., Carmichael, G., Chatfield, R., Connell, P., Derwent, R., Horowitz, L., Jin, S., Kanakidou, M., Kasibhatla, P., Kotamarthi, R., Kuhn, M., Law, K., Penner, J., Perliski, L., Sillman, S., Stordal, F., and Thompson, A., and Wild, O.: 1997, 'Results from the Intergovernental Panel on Climatic Change Photochemical Model Intercomparison (Photocomp)', *J. Geophys. Res.* **102**, 5979–5991.

Penner, J. E., Atherton, C. S., Dignon, J., Ghan, S. J., Walton, J. J., and Hameed, S.: 1991, 'Tropospheric Nitrogen: A Three-Dimensional Study of Sources, Distributions and Deposition', *J. Geophys. Res.* **96**, 959–990.

Prather, M. J.: 1994, 'Lifetimes and Eigenstates in Atmospheric Chemistry', *Geophys. Res. Lett.* **21**, 801–804.

Prather, M. J.: 1996, 'Natural Modes and Time Scales in Atmospheric Chemistry: Theory, GWPs for CH_4 and CO, and Runaway Growth', *Geophys. Res. Lett.* **23**, 2597–2600.

Ramanathan, V., Callis, L., Cess, R., Hansen, J., Isaksen, I., Kuhn, W., Lacis, A., Luther, F., Mahlman, J., Reck, R., and Schlesinger, M.: 1987, 'Climate-Chemical Interactions and Effects of Changing Atmospheric Trace Gases', *Rev. Geophys.* **25**, 1441–1482.

Rasch, P. J., Feichter, J., Law, K., Mahowald, N., Penner, J., Benkowitz, C., Genthon, C., Giannakopoulos, C., Kasibhatla, P., Koch, D., Levy, H., Maki, T., Prather, M., Roberts, D. L., Roelofs, G.-J., Stevenson, D., Stockwell, Z., Taguchi, S., Kritz, M., Chipperfield, M., Baldocchi, D., McMurray, P., Barrie, L., Balkanski, Y., Chatfield, R., Kjellstrom, E., Lawrence, M., Lee, H. N., Lelieveld, J., Noone, K. J., Seinfeld, J., Stenchikov. G., Schwartz, S., Walcek, C., and Williamson, D.: 2000, 'A Comparison of Scavenging and Deposition Processes in Global Models: Results from the WCRP Cambridge Workshop of 1995', *Tellus* **52B**, 1025–1056.

Stevenson, D. S., Collins, W. J., Johnson, C. E., and Derwent, R. G.: 1998, 'Intercomparison and Evaluation of Atmospheric Transport in a Lagrangian Model (STOCHEM), and an Eulerian Model (UM), Using ^{222}Rn as a Short-Lived Tracer', *Quart. J. Roy. Meteorol. Soc.* **124**, 2477–2491.

Stevenson, D. S., Johnson, C. E., Collins, W. J., Derwent, R. G., Shine, K. P., and Edwards, J. M.: 1998, 'Evolution of Tropospheric Ozone Radiative Forcing', *Geophys. Res. Lett.* **25**, 3819–3822.

Walton, J., MacCracken, M., and Ghan, S.: 1988, 'A Global-Scale Lagrangian Trace Species Model of Transport, Transformation, and Removal Processes', *J. Geophys. Res.* **93**, 8339–8354.
Wild, O. and Prather, M. J.: 2000, 'Excitation of the Primary Tropospheric Chemical Mode in a Global Three-Dimensional Model', *J. Geophys. Res.* **105**, 24647–24660.

(Received 19 December 2000; in revised form 6 July 2001)